Since January 2020 Elsevier has created a COVID-19 resource centre with free information in English and Mandarin on the novel coronavirus COVID-19. The COVID-19 resource centre is hosted on Elsevier Connect, the company's public news and information website.

Elsevier hereby grants permission to make all its COVID-19-related research that is available on the COVID-19 resource centre - including this research content - immediately available in PubMed Central and other publicly funded repositories, such as the WHO COVID database with rights for unrestricted research re-use and analyses in any form or by any means with acknowledgement of the original source. These permissions are granted for free by Elsevier for as long as the COVID-19 resource centre remains active.

Articles

Newly discovered coronavirus as the primary cause of severe acute respiratory syndrome

Thijs Kuiken, Ron A M Fouchier, Martin Schutten, Guus F Rimmelzwaan, Geert van Amerongen, Debby van Riel, Jon D Laman, Ton de Jong, Gerard van Doornum, Wilina Lim, Ai Ee Ling, Paul K S Chan, John S Tam, Maria C Zambon, Robin Gopal, Christian Drosten, Sylvie van der Werf, Nicolas Escriou, Jean-Claude Manuguerra, Klaus Stöhr, J S Malik Peiris, Albert D M E Osterhaus

Summary

Background The worldwide outbreak of severe acute respiratory syndrome (SARS) is associated with a newly discovered coronavirus, SARS-associated coronavirus (SARS-CoV). We did clinical and experimental studies to assess the role of this virus in the cause of SARS.

Methods We tested clinical and postmortem samples from 436 SARS patients in six countries for infection with SARS-CoV, human metapneumovirus, and other respiratory pathogens. We infected four cynomolgus macaques (*Macaca fascicularis*) with SARS-CoV in an attempt to replicate SARS and did necropsies on day 6 after infection.

Findings SARS-CoV infection was diagnosed in 329 (75%) of 436 patients fitting the case definition of SARS; human metapneumovirus was diagnosed in 41 (12%) of 335, and other respiratory pathogens were diagnosed only sporadically. SARS-CoV was, therefore, the most likely causal agent of SARS. The four SARS-CoV-infected macaques excreted SARS-CoV from nose, mouth, and pharynx from 2 days after infection. Three of four macaques developed diffuse alveolar damage, similar to that in SARS patients, and characterised by epithelial necrosis, serosanguineous exudate, formation of hyaline membranes, type 2 pneumocyte hyperplasia, and the presence of syncytia. SARS-CoV was detected in pneumonic areas by virus isolation and RT-PCR, and was localised to alveolar epithelial cells and syncytia by immunohistochemistry and transmission electron microscopy.

Interpretation Replication in SARS-CoV-infected macaques of pneumonia similar to that in human beings with SARS, combined with the high prevalence of SARS-CoV infection in SARS patients, fulfill the criteria required to prove that SARS-CoV is the primary cause of SARS.

Lancet 2003; **362:** 263–70. Published online July 22, 2003
http://image.thelancet.com/extras/03art6318web.pdf

Departments of Virology (T Kuiken PhD, R A M Fouchier PhD, M Schutten PhD, G F Rimmelzwaan PhD, G van Amerongen, G van Doornum PhD, A D M E Osterhaus PhD), **Immunology** (D van Riel, J D Laman PhD), **and Pathology** (T de Jong), **Erasmus Medical Centre, PO Box 1738, 3000 DR Rotterdam, Netherlands; Government Virus Unit, Public Health Laboratory Centre, Shek Kip Mei, Kowloon, Hong Kong Special Administrative Region, China** (W Lim MD); **Department of Pathology, Singapore General Hospital, Singapore** (A E Ling FRCPA); **Department of Microbiology, Chinese University of Hong Kong, Prince of Wales Hospital, Hong Kong** (P K S Chan MD, J S Tam PhD); **Enteric Respiratory and Neurological Virus Laboratory, Health Protection Agency, London, UK** (M C Zambon PhD, R Gopal PhD); **Department of Virology, Bernhard-Nocht Institute for Tropical Medicine, Hamburg, Germany** (C Drosten MD); **Unité de Génétique Moléculaire des Virus Respiratoires, Institut Pasteur, Paris, France** (S van der Werf PhD, N Escriou PhD, J-C Manuguerra PhD); **SARS Aetiology Study Group, WHO, Geneva, Switzerland** (K Stöhr PhD); **and Department of Microbiology and Medicine, Queen Mary Hospital, University of Hong Kong** (J S M Peiris DPhil)

Correspondence to: Dr Thijs Kuiken
(e-mail: t.kuiken@erasmusmc.nl)

Introduction

Severe acute respiratory syndrome (SARS) is an emergent disease that was first reported in Guangdong Province, People's Republic of China, in November, 2002, from where it spread to other Asian countries, North America, and Europe.[1–5] By July 3, 2003, this epidemic had resulted globally in 8439 reported cases, of which 812 were fatal.[6]

Pulmonary lesions in SARS patients have been diagnosed as diffuse alveolar damage. Histological changes include desquamation of pneumocytes, formation of hyaline membranes, flooding of alveolar lumina with oedema fluid mixed with inflammatory cells, and the presence of enlarged pneumocytes and syncytia. Alveolar walls are thickened by mild mononuclear infiltrate, and in later stages air spaces contain fibromyxoid-organising exudate.[2,4,5,7,8] Coronavirus-like particles have been detected by transmission electron microscopy in cells from a lung biopsy sample[2] and a bronchoalveolar lavage sample,[7] and in pneumocytes from a postmortem lung sample.[8] Until now, immunohistochemical detection of SARS-associated coronavirus (SARS-CoV) in SARS-associated lesions has not succeeded.[7]

Identification of the causal agent of SARS is essential to make an accurate case definition, to diagnose the disease accurately, and to develop appropriate preventive and curative treatment. Several agents have been proposed in the course of investigation of SARS. During initial investigations in China, *Mycoplasma pneumoniae* and *Chlamydia* sp were suggested as possible causes.[9,10] Subsequent studies ruled out these agents and other known viral and bacterial pathogens,[3,4] except for human metapneumovirus.[5] A previoulsy unknown coronavirus was identified in patients with SARS.[2,7,11] It was suggested that this coronavirus, alone or in combination with human metapneumovirus or other causal agents, might be the primary cause of SARS.

We investigated the causal role of the newly discovered SARS-CoV by analysis of the results of investigations done by the WHO network of laboratories, showing that SARS-CoV was the only agent seen consistently in patients with probable SARS. We also investigated whether respiratory lesions of SARS could be replicated in experimentally infected cynomolgus macaques (*Macaca fascicularis*). Replication was based on histopathology, as in a preliminary report,[12] and on localisation of SARS-CoV to the typical pulmonary lesions by immunohistochemistry and transmission electron microscopy.

For personal use. Only reproduce with permission from The Lancet.

	Date of admission (day/month)	Location	Hospital identification
Cohort (n)			
1 (50)	26/2 to 26/3	Hong Kong	3 hospitals
2 (75)	24/3 to 28/3	Hong Kong	1 hospital
3 (6)	··*	Hong Kong	Kowloon cluster of hospitals
4 (84)	4/3 to 19/3	Hong Kong	Prince of Wales Hospital
5 (8)	22/2 to 28/2	Hong Kong	Hospitals A to C
6 (14)	4/4 to 7/4	Hong Kong	Hospital D
7 (26)	12/3 to 15/4	Hong Kong	Hospital E
8 (199)	1/3 to 22/4	Singapore	Tan Tock Seng Hospital, Singapore General Hospital
9 (3)	15/3 to 4/4	Germany	University Hospital of Frankfurt/Main, Hattingen Hospital, Hemer Hospital
10 (9)†	17/3 to 10/4	UK	9 hospitals in England and Scotland
11 (17)	4/3 to 20/3	Vietnam	French Hospital, Hanoi
12 (19)‡	20/3 to 22/4	France	9 hospitals

*Fatal cases from March. †All fitted WHO definition of probable SARS case and had recently returned from Hong Kong, China, Singapore, Vietnam, or Taiwan. ‡Five probable and 14 suspected SARS cases.

Table 1: **Origin of patients fitting WHO case definition for SARS**

Methods

Investigations on SARS patients

All patients in this study fitted the WHO case definition for SARS (table 1).[1] Some of the data on various proportions of patients in cohorts 1,[2] 2,[13] 3,[8] 5–8,[7] and 9, 11, and 12[11] have been published previously.

Antibody to SARS-CoV was detected in paired acute and convalescent sera by use of an indirect immunofluorescence assay[2] for patients in all cohorts. In addition, an enzyme-linked immunosorbent assay[7] was used with minor modifications in cohorts 8 and 10. Antibody to human metapneumovirus was detected in paired acute and convalescent sera by use of an immunofluorescence assay on human-metapneumovirus-infected fetal rhesus monkey kidney (FRhK-4) cells[14] for 32 patients in cohort 1, and for all patients who were human-metapneumovirus culture positive in cohorts 3 and 4. IgA-specific and IgG-specific EIA were used for the remaining five patients in cohort 1, and for all patients in cohort 8. An IgA-specific EIA was used for patients in cohort 5. These tests are under development for commercial distribution (Meddens Diagnostics, Vorden, Netherlands).

The clinical samples from which RNA extracts were obtained varied among cohorts and included swabs from nose, pharynx, or conjunctiva, aspirates from nasopharynx or trachea, bronchoalveolar lavage fluid, faeces, urine, sputum, and blood. Samples included postmortem lung tissue in cohort 3, and from various organs in cohort 8. The RT-PCR for SARS-CoV on clinical samples was done according to Peiris and colleagues' method[2] for cohorts 1–3, and according to that by Drosten and colleagues[11] for cohorts 9, 11, and 12. Comparable tests that used primer pair COR-1/COR-2 were used for cohorts 5–7,[15] primer pairs Cor-p-F3/Cor-p-R1 and 2Bp/4Bm for cohort 10,[15,16] and primer pairs COR-1/COR-2 and SAR1s/SAR1 as for cohort 8.[15] Virus isolation procedures for SARS-CoV were done by inoculation of samples on to Vero cells for cohorts 4–7, and on to HeLa, human embryonic lung, LLC, Madin-Darby canine kidney cells, and Vero cell lines for cohort 8. Presence of virus was confirmed by immunofluorescence, RT-PCR, or both.

The RT-PCR for human metapneumovirus on clinical samples was done according to Peiris and colleagues' method[2] for cohorts 1 and 3, with use of primer pair L6 (5′-CATGCCCACTATAAAAGGTCAG-3′) and L7 (5′-CACCCCAGTCTTTCTTGAAA-3′) for cohorts 5–7, according to the method of Peret and colleagues,[17] with conventional and real-time PCR for cohort 8, with use of a family-specific primer pair according to Drosten and colleagues[11] for cohort 9, for cohort 10 with use of N and F gene-based primers, and by nested PCR with use of the outer primer pair P9 (5′-GATCAACATATCT TCAGTCCAGAC-3′) and P10 (5′-AAAAGCATGATC CGATATGAACCC-3′) and L6 and L7 as inner primer pair for cohorts 11 and 12. In addition, for cohort 8 samples were inoculated onto HeLa, human embryonic lung, LLC, Madin-Darby canine kidney, and Vero cell lines for 28 days at 33°C.

For cohort 4, nasopharyngeal aspirate samples were inoculated onto LLC-MK2 rhesus monkey kidney cell and human laryngeal carcinoma cell (HEp-2) monolayers and incubated at 37°C for 12–14 days (HEp-2 cells) or 21 days (LLC-MK2 cells) in a roller tube culture system. These cell lines were selected based on the results of an initial assessment.[18] Irrespective of the presence of cytopathic effect, cell culture supernatants were testd for human metapneumovirus by nested RT-PCR with use of the outer primer pair (5′-AGCTGTTCCATTGG CAGCA-3′) and (5′-ATGCTGTTCRCCYTCAAC TTT-3′; R=A or G, Y=C or T) and the inner primer pair (5′-GAGTAGGGATCATCAAGCA-3′) and (5′-GCT TAGCTGRTATACAGTGTT-3′). All PCR products were confirmed by nucleotide sequencing. In addition, all cell cultures positive for human metapneumovirus rtPCR were passaged on to another LLC-MK2 rhesus monkey kidney cell culture tube and incubated for 21 days. Randomly selected supernatants of cell cultures with cyopathic effect were examined by electron microscopy for the presence of virus particles.

Macaque investigations

We made the virus stock used to inoculate cynomolgus macaques from the fourth passage of a SARS-CoV isolate, obtained from patient 5688, who died of SARS, and inoculated it on to Vero 118 cells cultured in Iscove's Modified Dulbeco's Medium (Bio Whitaker, Walkersville, MD, USA). After centrifugation at 270 *g* for 5 min, 1 mL samples were made from the supernatant and from the pelleted cells, which were resuspended in 5 mL medium. The titre of this virus stock was 1×10^6 median tissue culture infectious dose ($TCID_{50}$) per mL. All cell cultures were done under biosafety level 3 conditions.

Four adult cynomolgus macaques, two males and two females, were placed in negatively pressurised glove boxes. They were infected with 1×10^6 $TCID_{50}$ of SARS-CoV suspended in 5 mL phosphate-buffered saline. 4 mL was applied intratracheally, 0·5 mL intranasally, and 0·25 mL on each conjunctiva. We checked the macaques daily for clinical signs. Just before infection and at days 2, 4, and 6 after infection, we anaesthetised the macaques with ketamine and collected 10 mL blood from inguinal veins, and took nasal, oral, pharyngeal, and rectal swabs, which were placed in 1 mL virus transport medium.[19] From macaques 3 and 4, we also collected sputum samples by use of swabs under the tongue and sponges placed in the buccal cavity during anaesthesia. We extracted fluid from the sponges by centrifugation. The macaques were euthanised 6 days after infection by exsanguination under ketamine anesthesia.

We did necropsies of the macaques according to a standard protocol. For histological examination we collected the following tissues: adrenal gland, aorta, axillary lymph node, brachial biceps muscle, brain stem, caecum, cerebellum, cerebrum, colon, duodenum, eye,

For personal use. Only reproduce with permission from The Lancet.

eyelid, femoral bone marrow, heart muscle (left and right), ileum, inguinal lymph node, jejunum, kidney, lung (inflated with 10% neutral-buffered formalin), liver, mandibular lymph node, mesenteric lymph node, nasal septum, oesophagus, pancreas, primary bronchus, ovary, prostate, salivary gland, skin, spleen, stomach, testis, thymus, thyroid gland, tongue, tonsil, trachea, tracheobronchial lymph node, urinary bladder, and uterus. Tissues for light-microscope examination were fixed in 10% neutral-buffered formalin, embedded in paraffin, and 4 μm sections were stained with haematoxylin and eosin. Selected lung sections were stained with monoclonal antibody AE1/AE3 (Neomarkers, Fremont, CA, USA) for the identification of epithelial cells, and monoclonal antibody CD68 (Dako, Glostrup, Denmark) for the identification of macrophages according to standard immunohistochemical procedures.

We developed an immunohistochemical method for detecting SARS-CoV antigen. Duplicate sections of all tissue samples were stained with an avidin-biotin complex peroxidase method. Paraffin was removed from sections, which were rehydrated and pretreated with protease (Sigma, St Louis, MO, USA) for 10 min at 37°C. Endogenous peroxidase was revealed with 4-chloro-1-naphthol (Sigma). Endogenous biotin was blocked with an avidin-biotin blocking kit (Vector Laboratories, Burlingame, CA, USA). Slides were briefly washed with 0·05% phosphate-buffered saline Tween 20 (Fluka, Buchs, Switzerland) and incubated with biotinylated purified human IgG from a convalescent SARS patient, negative control biotinylated purified human IgG, or the dilution buffer (phosphate-buffered saline containing 1% bovine serum albumin) for 1 h at room temperature. After washing, sections were incubated with avidin-biotin complex-horseradish peroxidase (Dako) for 1 h at room temperature. Horseradish peroxidase activity was revealed by incubating slides in 3-amino-9-ethylcarbazole (Sigma) solution for 10 min, resulting in a bright red precipitate. Sections were counterstained with haematoxylin. Tissue sections from cynomolgus macaques that had not been infected with SARS-CoV were included as negative controls. We included formalin-fixed, paraffin-embedded SARS-CoV-infected or uninfected Vero 118 cells in each staining as positive and negative controls, respectively.

For negative contrast electron microscopy, samples of tissue culture supernatants were centrifuged at 17 000 *g* at 4°C, after which the pellet was resuspended in phosphate-buffered saline and stained with phosphotungstic acid. Samples of lung from macaque 3 were fixed for transmission electron microscopy in 4% formaldehyde and 1% glutar(di)aldehyde after brief fixation in 10% neutral-buffered formalin, and post-fixed in 1% osmium tetroxide. After embedding in epoxy resin, thin sections were prepared, stained with 6% saturated uranyl acetate and lead citrate, and examined with a Philips Morgagni 268D electron microscope.

Samples from lung, duodenum, jejunum, kidney, liver, and spleen were collected post mortem for virus isolation and RT-PCR. Additionally, we collected the following samples for RT-PCR only: cerebellum, cerebrum, ileum, intestinal contents from the colon, mesenteric lymph node, nasal septum, pancreas, skin, spleen, stomach, tonsil, trachea, tracheobronchial lymph node, urinary bladder, and urine. From macaques 3 and 4, samples of intestinal contents from the jejunum, ileum, and caecum were also collected for RT-PCR. Intestinal contents were pretreated with stool transport and recovery buffer (Roche Diagnostics, Mannheim, Germany) before further processing. Tissue samples were homogenised in 4 mL transport medium[19] with Polytron PT2100 tissue grinders (Kinematica, Littau-Lucerne, Switzerland). After low-speed centrifugation, the homogenates were frozen at –70°C until inoculation on Vero 118 cell cultures in logarithmic dilutions. The infectious virus titres were expressed as $TCID_{50}$/g of tissue. The identity of the isolated virus was confirmed as SARS-CoV by RT-PCR of supernatant.

We developed an RT-PCR with primers and probe specific for the nucleoprotein gene of SARS-CoV because the nature of the coronavirus replication cycle[20] suggested that such an assay may be more sensitive than RT-PCRs based on the polymerase gene, which are currently in use for diagnostics. Nucleic acid isolation was done on the Magnapure LC automated nucleic acid isolation system (Roche Diagnostics). Swabs, faeces, and serum were processed with the Magnapure LC total nucleic acid serum plasma blood isolation kit. Postmortem tissue samples were processed with the Magnapure LC RNA isolation kit I on the Magnapure LC station using the external lysis protocol. SARS-CoV RNA was detected on the ABI prism 7700, with use of the EZ rTtH RNA amplification kit (Applied Biosystems, Foster City, CA, USA). Primers SARSNP fpr1 (5′-CAAACATTGGCCG CAAATT-3′), SARSNP rpr1 (5′-CAATGCGTGACA TTCCAAAGA-3′), and probe SARSNP prb1 (5′-CACAATTTGCTCCAAGTGCCTCTGCA-3′) (Eurogentec) specific for the nucleoprotein (*NP*) gene of SARS-CoV were used for amplification. Amplification parameters were 2 min at 50°C, 30 min at 60°C, 5 min at 95°C, and 45 cycles of 30 s at 95°C, and 1 min at 62°C.

We compared the sensitivity of the SARS-CoV *NP* rtPCR with a SARS-CoV polymerase rtPCR that used essentially the same methods with primers and probe specific for the SARS-CoV polymerase (SARSTM fpr1 5′-TGTGCGCAAGTATTAAGTGAGATG-3′, SARSTM rpr1 5′-CACCGGATGATGTTCCACC-3′, SARSTM prb1 5′-FAMTCATGTGTGGCGGCTCA CTATATGTTAAACC-TAMRA-3′). Serial dilutions of the SARS-CoV virus stock and SARS-CoV-infected Vero cells from patient 5688 were made and tested with the *NP* and polymerase-specific RT-PCRs.

Samples from the respiratory tract (nasal swabs, pharyngeal swabs, postmortem trachea, and lung samples) were also monitored for influenza A and B virus, respiratory syncytial virus A and B, rhinovirus, coronavirus (OC43 and 229E), and human metapneumovirus with use of essentially the same RT-PCR methods but with specific primers.

We detected antibody to SARS-CoV in macaque sera by use of an indirect immunofluorescence assay. SARS-CoV-infected Vero 118 cells that had developed cytopathic effect were used to coat microscope slides. After incubation of the serum for 30 min at 37°C, slides were washed with phosphate-buffered saline and incubated with antihuman IgG, IgA, and IgM, conjugated with fluorescein thiocyanate (Dako). After washing and drying, slides were examined with a fluorescence microscope (Zeiss Axioscope, Oberkochen, Germany).

We tested lung swabs and blood samples for bacterial pathogens at the Department of Medical Microbiology and Infectious Diseases, Erasmus MC, Rotterdam, Netherlands, by routine bacteriological methods (with blood agar, chocolate agar, and MacConkey agar) under aerobic and anaerobic conditions. Lung-tissue homogenates were tested for the presence of *Chlamydia pneumoniae* with PCR using universal primers for *Chlamydia* sp[21] and specific primers for *C pneumoniae*.[22]

For personal use. Only reproduce with permission from The Lancet.

Cohort number	Origin	SARS-CoV			hMPV		
		Number with serological results (n/total)	Number with virological results (n/total)	Total number with results (n/total [%])	Number with serological results (n/total)	Number with virological results (n/total)	Total number with results (n/total [%])
1	Hong Kong	32/32	34/46	45/50	0/32	0/50	0/50 (0)
2	Hong Kong	70/75	69/75	70/75 (93)	ND	ND	ND
3	Hong Kong	6/6	5/6	6/6 (100)	0/6	0/6	0/6 (0)
4	Hong Kong	84/84	84/84*	84/84 (100)	30/84	30/84†‡	30/84 (36)
5	Hong Kong	8/8	8/8‡	8/8 (100)	1/7	0/8	1/8 (13)
6	Hong Kong	9/9	14/14‡	14/14 (100)	ND	2/14	2/14 (14)
7	Hong Kong	1/1	15/26‡	15/26 (58)	ND	2/26	2/26 (8)
8	Singapore	48/50	23/94	68/125 (54)	2/59	0/85	2/116 (2)
9	Germany	3/3	3/3	3/3 (100)	ND	0/2	0/2 (0)
10	UK	1/9	1/9	1/9 (11)§	ND	0/9	0/9 (0)
11	Vietnam	ND	11/17	11/17 (65)	ND	1/10	1/10 (10)
12	France	2/5¶	3/19	4/19 (21)‖	ND	3/10	3/10 (30)**
Total		264/282	270/401	329/436 (75)	33/188	38/304	41/335 (12)

hMPV=human metapneumovirus. ND=not done. *All positive Vero cell cultures also showed cytopathic effect 2–3 days after passage on to another Vero cell culture tube. †Nucleotide sequence of all RT-PCR products identical to F gene fragment of a published hMPV strain with GenBank accession number NC 004148; reference 24. Inoculation of all hMPV RT-PCR-positive cell cultures on to another LLC-MK2 cell culture tube resulted in similar cytopathic effect, characterised by focal refractile rounding of cells that progressed slowly to cell detachment. By electron microscopy, hMPV particles were seen in all five randomly selected cell culture supernatants. ‡15 coronavirus isolates obtained from these RT-PCR positive patients. §Of eight patients not diagnosed with SARS-CoV infection, three diagnosed with influenza, one with *M pneumoniae* infection, and one with *Legionella* sp infection. ¶All five we've tested probable SARS patients. ‖All four patients were probable SARS cases. **All three patients suspected SARS cases. Of suspect SARS cases, two of 12 tested positive for influenza A virus (H3).

Table 2: **Diagnosis of SARS-CoV and human metapneumovirus in patients fitting the WHO SARS case definition**

Role of the funding source

The sponsors of the study had no role in the study design, data collection, data analysis, data interpretation, or in the writing of the report.

Results

Overall, 75% of patients who had suspected SARS according to the WHO case definition were diagnosed as being infected with probable SARS-CoV, whereas 12% were diagnosed as having human metapneumovirus infection (table 2). The high proportion of patients diagnosed with human metapneumovirus infection could be attributed mainly to cohort 4, in which 36% of patients were positive for this infection. Without this cohort, the overall proportion of human metapneumovirus diagnoses decreased to 4%. Alternative diagnoses in patients who tested negative for SARS-CoV infection were influenza (five), *M pneumoniae* infection (one), and *Legionella* sp infection (one).

Three macaques (1, 2, and 4) became lethargic from days 2–3 after infection onwards. Macaques 1 and 2 developed a temporary skin rash at day 4 after infection. Macaque 2 had respiratory distress, consisting of an increased respiratory rate and dyspnoa, from day 4 after infection onwards. Macaques 2–4 had multiple foci of pulmonary consolidation in both lungs. The consolidated lung tissue was grey-red, firm, level, and less buoyant than normal. The tracheobronchial lymph nodes and spleen in these macaques were about twice the normal size. The other organs in these three macaques, as well as the respiratory tract and other organs of macaque 1 were normal on microscopic inspection.

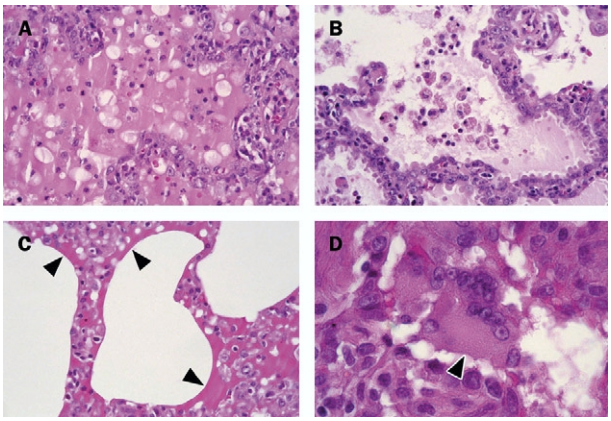

Figure 1: **Histological lesions in lungs from cynomolgus macaques infected with SARS-CoV**

A: Early changes of diffuse alveolar damage, characterised by disruption of alveolar walls and flooding of alveolar lumina with serosanguineous exudate admixed with neutrophils and alveolar macrophages. B: More advanced changes of diffuse alveolar damage, characterised by thickened alveolar walls lined by type 2 pneumocytes, and mainly alveolar macrophages in alveolar lumina. C: Arrows show hyaline membranes on surfaces of alveoli. D: A characteristic change is presence of syncytia (arrowhead), here in the lumen of bronchiole. All slides haematoxylin and eosin stained.

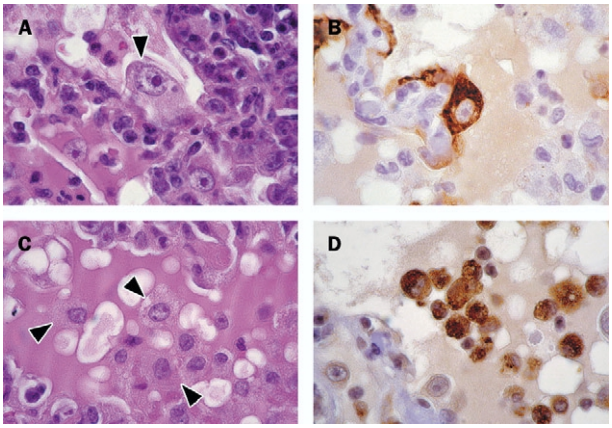

Figure 2: **Immunohistochemical identification of cells in lungs from cynomolgus macaques infected with SARS-CoV**

A: Arrows show enlarged type 2 pneumocytes with abundant vesicular cytoplasm and large nucleus containing prominent nucleolus that frequently occur along alveolar walls; haematoxylin and eosin. B: Epithelial origin confirmed by positive staining with monoclonal antibody AE1/AE3, a pan-keratin marker; avidin-biotin complex immunoperoxidase with diaminobenzidine substrate and hematoxylin counterstain. C: Arrows show alveolar macrophages that are common in alveolar lumina; haematoxylin and eosin. D: Macrophage origin is confirmed by positive staining with monoclonal antibody CD68, a macrophage marker; avidin-biotin complex immunoperoxidase with diaminobenzidine substrate and haematoxylin counterstain.

For personal use. Only reproduce with permission from The Lancet.

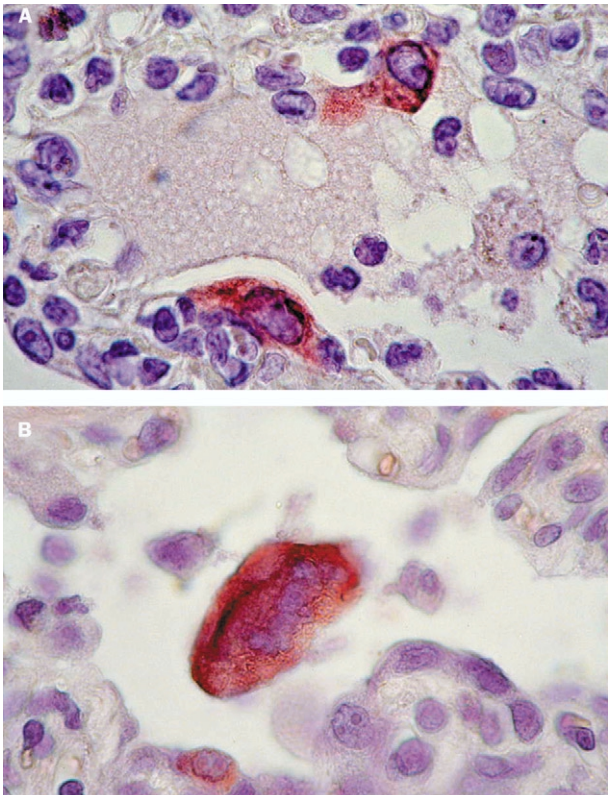

Figure 3: **Immunohistochemical detection of SARS-CoV in lungs from experimentally infected cynomolgus macaques**
A: Expression of SARS-CoV antigen by two alveolar epithelial cells, probably type 2 pneumocytes. Immunoglobulin G fraction of convalescent serum of SARS patient was used as specific antibody; avidin-biotin complex immunoperoxidase with diaminobenzidine substrate and haematoxylin counterstain. B: Expression of SARS-CoV antigen by syncytium in lumen of alveolar duct. Small cell along the duct wall also stains positive; avidin-biotin complex immunoperoxidase with 3-amino-9-ethylcarbazole substrate and haematoxylin counterstain.

The main lesion in the consolidated pulmonary tissue of macaques 2–4 involved the alveoli and bronchioles, and consisted of areas with acute or more advanced phases of diffuse alveolar damage. In such areas the lumina of alveoli and bronchioles were variably filled with protein-rich oedema fluid, fibrin, erythrocytes, and cellular debris, a moderate number of alveolar macrophages, and fewer neutrophils and lymphocytes (figure 1). The cytoplasm of some of these macrophages contained erythrocytes or pools of oedema fluid. There was extensive loss of epithelium from alveolar and bronchiolar walls. In areas with more advanced diffuse alveolar damage, the alveolar walls were moderately thickened and lined by cuboidal epithelial cells (type 2 pneumocyte hyperplasia), and the alveolar lumina contained mainly alveolar macrophages (figure 1). Regeneration of epithelium was seen in some bronchioles, visible as one irregular layer of squamous to high cuboidal epithelial cells with hyperchromatic nuclei. In some areas, the alveolar walls were lined by deep eosinophilic hyaline membranes (figure 1). There were occasional multinucleated giant cells (syncytia) in bronchioles and alveoli, either attached to the wall or free in the lumen (figure 1). These syncytia had up to about 30 peripheral nuclei, abundant hyaline eosinophilic cytoplasm, and, based on positive CD68 staining and negative pan-keratin staining, originated from marcophages. Enlarged type 2 pneumocytes with large vacuolated nuclei, prominent nucleoli and abundant vesicular cytoplasm were frequently found attached to the alveolar walls (figure 2). The epithelial origin of these cells was confirmed by keratin expression (figure 2). By contrast, alveolar macrophages had smaller nuclei, less prominent nucleoli, and were generally loose in the alveolar lumina (figure 2). The identity of these cells as macrophages was confirmed by CD68 staining (figure 2). Alveolar and bronchiolar walls were thickened by oedema fluid, mononuclear cells, and neutrophils. There were aggregates of lymphocytes around small pulmonary vessels. Moderate numbers of lymphocytes and macrophages were present in the lamina propria and submucosa of the bronchial walls, and a few neutrophils in the bronchial epithelium.

Changes in other tissues of macaques 2–4 were diffuse lymphoid hyperplasia and sinus histiocytosis of the tracheobronchial lymph nodes. Macaques 2 and 3 also had diffuse intrafollicular hyalinosis of the spleen. There were minimum multifocal inflammatory lesions in the pulmonary tissue of macaque 1, consisting of increased numbers of alveolar macrophages (about ten per alveolus) and occasional syncytia in alveoli and bronchioles.

With use of a biotinylated IgG fraction from a SARS patient, SARS-CoV expression was detected in a few to moderate numbers of alveolar epithelial cells (type 2 pneumocytes; figure 3) and rare intrabronchiolar and intra-alveolar syncytia (figure 3) in inflamed lung tissue of macaques 2–4. Positive immunohistochemical staining for SARS-CoV was visible as diffuse red-brown staining in the cytoplasm. The character of the staining was similar to that in SARS-CoV-infected Vero 118 cells (positive control), whereas non-infected Vero 118 cells and lung tissue from non-infected macaques (negative controls) were negative on staining. The other tissues in these three macaques, as well as the lung and other tissues of macaque 1, showed no SARS-CoV expression by immunohistochemistry.

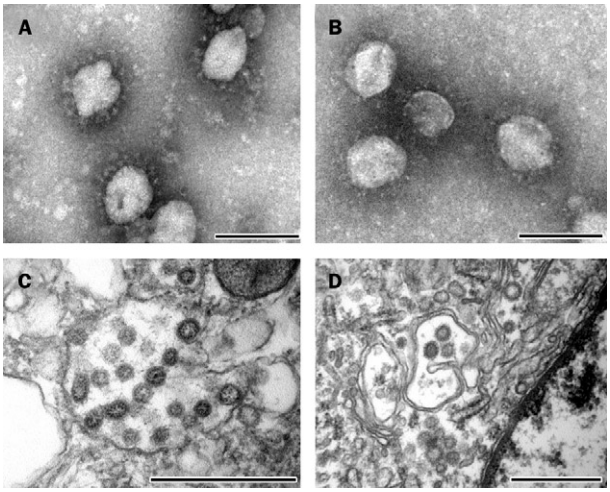

Figure 4: **Electron microscopy of SARS-CoV in inoculum, clinical samples, and tissue samples of experimentally infected cynomolgus macaques**
A: Negative-contrast electron microscopy of virus stock used to inoculate cynomolgus macaques shows the typical club-shaped surface projections of coronavirus particles; negatively stained with phosphotungstic acid, bar=100 nm. B: Morphologically identical particles isolated from nasal swabs of infected macaques; negatively stained with phosphotungstic acid, bar=100 nm. C: Transmission electron microscopy of infected Vero 118 cell shows viral nucleocapsids with variably electron-dense and electron-lucent cores in smooth-walled vesicles in the cytoplasm; stained with uranyl acetate and lead citrate, bar=500 nm. D: Morphologically similar particles occur in pulmonary lesions of infected macaques, within vesicles of the Golgi apparatus of pneumocytes; stained with uranyl acetate and lead citrate; bar=500 nm.

For personal use. Only reproduce with permission from The Lancet.

	Time after infection (days)			
	0	2	4	6
Macaque number				
Sputum samples				
1	ND	ND	ND	ND
2	ND	ND	ND	ND
3	–	–	–	–
4	–	+	+	+
Nasal swab				
1	–	+	+	–
2	–	+	+	+
3	–	–	–	–
4	–	–	–	–
Pharyngeal swab				
1	–	+	–	+
2	–	+	+	+
3	–	–	–	–
4	–	+	+	+
Rectal swab				
1	–	–	–	–
2	–	–	–	–
3	–	–	–	–
4	–	–	–	–

Results from RT-PCR or virus isolation. ND=not done.

Table 3: **Excretion of SARS-CoV by experimentally inoculated cynomolgus macaques**

Ultrastructurally, coronavirus-like particles measuring about 70 nm in diameter with typical internal nucleocapsid-like structure and club-shaped surface projections were found in enlarged alveolar epithelial cells (type 2 pneumocytes) of inflamed lung tissue from macaque 3. The particles were localised within smooth-walled vesicles, often closely associated with the Golgi apparatus (figure 4). The particles in inflamed lung tissue were similar in size and structure to coronavirus particles in Vero 118 cells infected with SARS-CoV (figure 4).

The *NP*-specific RT-PCR was about 100-fold more sensitive than the polymerase-gene-based RT-PCR on the virus stock and the infected cell dilution series. The *NP* RT-PCR also was more sensitive based on detection of viral RNA in samples obtained from the SARS-CoV-infected macaques (data not shown).

The macaques shed SARS-CoV from sputum, nose, and pharynx from 2 days after infection onwards (table 3). SARS-CoV was isolated from the nasal and throat swabs from macaque 2 at 2 days after infection, from the throat swabs of macaque 4 at days 2, 4, and 6 after infection, and from sputum samples of macaque 4 at days 2 and 6 after infection. The virus titre in these samples was not measured. Several other clinical samples were positive only by RT-PCR (table 3). By negative-contrast electron microscopy, coronavirus particles were seen in cell cultures obtained from nasal swabs (figure 4) and closely resembled those in the virus stock used to infect the macaques (figure 4). Virus was not detected in rectal swabs. SARS-CoV was isolated from the lung (1×10^5 $TCID_{50}$/g tissue) and kidney (1×10^3 $TCID_{50}$/g tissue) of macaque 2, and from the lung (1×10^4 $TCID_{50}$/g tissue) of macaque 4. No virus was isolated from the postmortem samples of macaques 1 or 3. Several other tissues were positive only by RT-PCR (table 4). No macaque had detectable antibody to SARS-CoV by day 6 after infection.

	Macaque number			
	1	2	3	4
Sample				
Cerebrum	+	–	–	–
Duodenum	–	+	–	–
Kidney	–	+	–	–
Lung	+	+	+	+
Nasal septum	–	+	–	–
Skin	+	–	–	–
Spleen	–	–	–	+
Stomach	–	+	–	–
Trachea	+	–	–	+
Tracheo-bronchial lymph node	–	+	–	+
Urinary bladder	+	–	–	–

Results by RT-PCR or virus isolation. Tissues not listed had negative results.

Table 4: **Virological detection of SARS-CoV in postmortem tissues of experimentally infected cynomolgus macaques**

Virological examinations of nasal and pharyngeal swabs, and tracheal and lung samples from all four macaques by RT-PCR for influenza A and B virus, respiratory syncytial virus A and B, rhinovirus, coronavirus (OC43 and 229E) and human metapneumovirus were negative.

No relevant pathogens were identified on bacteriological culture of lung and blood samples. The lung homogenates tested negative for *Chlamydia* sp and *C pneumoniae* by PCR.

Discussion

According to Koch's postulates, as modified by Rivers for virus diseases,[23] six criteria need to be fulfilled for a particular micro-organism to be the causal agent of a disease. Laboratory investigations of clinical and postmortem samples from SARS patients, as presented here and in earlier studies[2,5,7,11] already fulfilled the first three criteria—isolation of the virus from diseased hosts, cultivation in experimental hosts or host cells, and proof of filterability (to exclude larger pathogens). The results of our studies on SARS-CoV-infected macaques fulfill the remaining postulates—production of a comparable disease in the original host or a related species, and reisolation of the virus. Detection of a specific immune response to the virus after experimental infection was already reported.[12] Together, these findings prove that SARS-CoV is the primary cause of SARS.

The primary role of SARS-CoV in the cause of SARS is suggested by the cumulative studies at WHO laboratories, in which most SARS patients were diagnosed as having SARS-CoV infection, frequently in the absence of other respiratory pathogens. The most common co-infection in SARS patients was with human metapneumovirus. The SARS patients in cohort 4 co-infected with human metapneumovirus were mostly health-care workers from the same ward and who shared resting areas. The circulation of this infection among them during the SARS outbreak probably explains the frequency of the infection in cohort 4. Similarly, four SARS patients from Canada were infected with SARS-CoV and human metapneumovirus.[5] The clinical symptoms of human metapneumovirus infection vary from mild upper-respiratory-tract disease to severe bronchiolitis and pneumonia.[24] The possible role of human metapneumovirus infection in exacerbating SARS remains to be assessed.

Alternative diagnoses, such as influenza, were occasionally made among patients fitting the case definition of SARS but testing negative for SARS-CoV infection. On the basis of the current case definition, therefore, disease from SARS-CoV infection overlaps with respiratory illnesses of other causes. Alternative diagnoses are most likely in geographical areas where SARS is not endemic.

The pulmonary lesions in SARS-CoV-infected macaques are comparable to those in SARS patients,[2,4,5,7,8] and to those in other respiratory coronavirus infections, such as sialodacryoadenitis virus infection in rats,[25] and porcine respiratory coronavirus infection in pigs.[26]

For personal use. Only reproduce with permission from The Lancet.

Syncytia were found commonly in bronchioles, and less frequently in alveolar ducts and alveoli, of SARS-CoV-infected macaques. Syncytia also were prominent in the alveoli of SARS patients.[3,7,8] Based on expression of CD68 and pan-keratin, the syncytia were of histiocytic origin in macaques (this study), and of histiocytic or epithelial origin in SARS patients.[8] The formation of syncytia in these macaques may have been induced by SARS-CoV infection, because some syncytia were positive for SARS-CoV by immunohistochemistry, and the spike protein of coronavirus induces cell to cell fusion.[20] Pneumocytes showing cytomegaly, enlarged nuclei, and prominent nucleoli were common both in SARS-CoV-infected macaques (this study) and in SARS patients.[2,8] Such enlargement and cytologic atypia of hyperplastic type 2 pneumocytes occurs commonly in organising diffuse alveolar damage, and is non-specific.[27]

The development of a specific immunohistochemical test to identify SARS-CoV antigen in histological samples allowed us to assess the cell tropism of SARS-CoV infection in macaques. Expression of SARS-CoV in the lung was restricted to pneumonic areas and localised to the cytoplasm of type 2 pneumocytes and syncytia. The infection of type 2 pneumocytes by coronavirus was confirmed by transmission electron microscopy. These findings correspond to the detection of coronavirus-like particles in pneumocytes of a postmortem lung sample of a SARS patient,[8] and with the tropism of respiratory coronaviruses in pigs and rats for respiratory epithelium, and occasionally alveolar macrophages.[25,26]

On the basis of histological changes, SARS-CoV infection in the macaques primarily affected the epithelium of alveoli and bronchioles. At the time of euthanasia, 6 days after infection, most pneumonic areas showed early to advanced type 2 pneumocyte hyperplasia, indicating repair of alveolar walls after loss of type 1 pneumocytes. The temporal sequence of the histological changes corresponds with that of experimental infection with porcine respiratory coronavirus in pigs, in which acute changes (loss of epithelium, presence of macrophages and fibrin in airway lumina) were seen at days 2–6 after infection, and more advanced changes (type 2 pneumocyte hyperplasia, interstitial mononuclear cell infiltration) were seen from days 7–11 after infection.[26] Because diffuse alveolar damage from different causes follows a common pathway,[27,28] more chronic changes in these macaques probably would have included organisation of the intra-alveolar exudate, resulting in alveolar fibrosis and bronchiolitis obliterans, as seen in SARS patients who died later in the course of disease.[3–5] The development of fibrosis is dependent on the deposition of fibrin in the alveoli rather than on the continued presence of virus infection. Onset of fibrosis is a critical feature of chronic diffuse alveolar damage, because it leads to loss of alveolar function and is irreversible.[27]

In respiratory coronavirus infections in pigs and rats, viral infection of respiratory epithelium is maximum at days 3–4 after infection, and is no longer measurable by days 6–9.[25,29] The rapid disappearance of infected cells after initial infection might explain why SARS-CoV was not found in type 1 pneumocytes, and was only occasionally found in type 2 pneumocytes in these macaques. It also might decrease the chance of detecting SARS-CoV by immunohistochemistry in postmortem lung tissue of SARS patients who die after a protracted course of disease.

The lymphoid depletion of splenic follicles in experimentally infected macaques corresponds to that seen in a SARS patient[8] and in pigs infection with porcine respiratory coronavirus.[29] Based on these findings, together with the leucopenia observed in SARS patients,[2–5] we speculate that SARS-CoV infection suppresses immunity and may predispose infected hosts to secondary infections, such as in measles virus infection.[30]

Virological examination of clinical and postmortem samples of experimentally infected macaques indicates that the respiratory tract was the most important source of virus, as is probably the case in human beings.[13] Unlike in SARS patients,[13] SARS-CoV was not detected in urine or faeces of these macaques, although faeces did test positive in a previous experiment.[12] This finding may be partly explained by the early cut-off point of the experiment (6 days after infection), because SARS-CoV RNA was detected in the faeces of SARS patients in the late convalescent phase.[11] The sporadic detection by RT-PCR of SARS-CoV in the urinary bladder, stomach, duodenum, cerebrum, and spleen in infected macaques in the absence of evidence of viral replication—based on virus culture or immunohistochemistry—suggests overspill from other tissues, for example via blood. The isolation of SARS-CoV from the kidney of one macaque suggests viral replication at that site, but this theory could not be confirmed by immunohistochemistry.

The RT-PCR based on nucleoprotein primers proved to be about 100-fold more sensitive than the existing RT-PCR, based on polymerase primers. Presumably, this difference is due to the gradient in the transcription of coronavirus RNA, with high concentrations of nucleoprotein RNA and low concentrations of polymerase RNA.[20]

Collectively, these results of laboratory studies of SARS patients and experimental infections of macaques prove that the newly discovered SARS-CoV is the primary causal agent of SARS. Based on histopathological and immunohistochemical analysis of postmortem tissues of these macaques, SARS-CoV infection primarily affects epithelium of the lower respiratory tract, with potentially severe consequences for respiratory function.

Conflict of interest statement

None declared.

Contributors

T Kuiken and R A M Fouchier participated in the joint planning and coordination of the study. T Kuiken wrote the report and supervised and interpreted the pathology, immunohistochemistry, and electron microscopy components of the experimental infections. R A M Fouchier and M Schutten developed, supervised, and assessed the RT-PCR for SARS-CoV. G F Rimmelzwaan and G van Amerongen planned and carried out the infection experiments. D van Riel and J D Laman were involved in the design, execution, and assessment of the immunohistochemistry test to detect SARS-CoV in tissues. T de Jong did the electron microscopy and detected SARS-CoV in pneumocytes. G van Doornum supervised the virological analyses of samples from the experimental infections. K Stöhr participated as secretary of the WHO laboratory network on SARS diagnosis and played a substantial part in the initiation of the study. A D M E Osterhaus was the principal investigator and was responsible for the overall planning and coordination of the study. All other researchers were involved in the development, application, assessment of diagnostic tests on samples from SARS patients, or a combination of these.

Acknowledgments

We thank, at the Erasmus Medical Centre, Rotterdam, the staff of the histology and immunohistochemistry laboratories of the Department of Pathology for technical assistance; Alewijn Ott and Arjen van Vliet, Diagnostic Unit, Department of Medical Microbiology and Infectious Diseases, for bacteriological examination of macaque tissues; and Alex van Belkum and Liesbeth van der Zwaan, Department of Medical Microbiology and Infectious Diseases, for examination of macaque lung homogenates for chlamydia. We thank Theo Bestebroer,

For personal use. Only reproduce with permission from The Lancet.

Berend Niemeyer, Georgina Aron, and Judith Guldemeester for virological assistance; Rob van Herwijnen, European Veterinary Laboratory, Woerden, for purification and biotinylation of primary antisera for immunohistochemistry; Frank van der Panne for assistance with preparation of figures; A M Burguière for contributions to analysis of the data; S Azebi, C Batejat, G Coralie, B Crescenzo-Chaigne, F Fichenick, S Gerbaud, V Lorin, C Rousseaux, and M Tardy-Panit for technical assistance; N Tordo for the design of primers P9 and P10 and for helpful discussions; and F Freymuth for providing free the human metapneumovirus. We thank the French medical team, the medical staff of the Hanoi French Hospital, and the medical teams at the hospitals in Tourcoing, Besançon, Strasbourg, Bordeaux, Montpellier, Hôpital d'Instruction des Armées, Brest, Rennes, CHU Bichat Claude Bernard, Paris, and CHU Pitié-Salpétrière, Paris for providing the samples. We thank the staff of the Department of Pathology, Virology Section, Singapore General Hospital, who did the bulk of the investigations there; and the staff of the Defence Medical Research Institute, who did some of the stool PCR tests.

References

1 WHO. Severe acute respiratory syndrome (SARS). *Wkly Epidemiol Rec* 2003; **78:** 81–83.
2 Peiris JS, Lai ST, Poon LL, et al. Coronavirus as a possible cause of severe acute respiratory syndrome. *Lancet* 2003; **361:** 1319–25.
3 Lee N, Hui D, Wu A, et al. A major outbreak of severe acute respiratory syndrome in Hong Kong. *N Engl J Med* 2003; **348:** 1986–94.
4 Tsang KW, Ho PL, Ooi GC, et al. A cluster of cases of severe acute respiratory syndrome in Hong Kong. *N Engl J Med* 2003; **348:** 1977–85.
5 Poutanen SM, Low DE, Henry B, et al. Identification of severe acute respiratory syndrome in Canada. *N Engl J Med* 2003; **348:** 1995–2005.
6 Cumulative number of reported probable cases of severe acute respiratory syndrome (SARS). http://www.who.int/csr/sars/country/2003_07_03 (accessed July 8, 2003).
7 Ksiazek TG, Erdman D, Goldsmith CS, et al. A novel coronavirus associated with severe acute respiratory syndrome. *N Engl J Med* 2003; **348:** 1953–66.
8 Nicholls JM, Poon LLM, Lee KC, et al. Lung pathology of fatal severe acute respiratory syndrome. *Lancet* 2003; **361:** 1773–78.
9 Pneumonia-China (Guangdong). http://www.promedmail.org/pls/askus/f?p=2400:1202:4008890228509 76471::NO::F2400_P1202_CHECK_DISPLAY,F2400_P1202_PUB _MAIL_ID:X,20691 (accessed July 8, 2003).
10 Pneumonia-China (Guangdong). http://www.promedmail.org/pls/askus/f?p=2400:1202:4008890228509 76471::NO::F2400_P1202_CHECK_DISPLAY,F2400_P1202_PUB _MAIL_ID:X,20755 (accessed May 19, 2003).
11 Drosten C, Gunther S, Preiser W, et al. Identification of a novel coronavirus in patients with severe acute respiratory syndrome. *N Engl J Med* 2003; **348:** 1967–76.
12 Fouchier RA, Kuiken T, Schutten M, et al. Aetiology: Koch's postulates fulfilled for SARS virus. *Nature* 2003; **423:** 240.
13 Peiris JS, Chu CM, Cheng VCC, et al. Clinical progression and viral load in a community outbreak of coronavirus-associated SARS pneumonia: a prospective study. *Lancet* 2003; **361:** 1767–72.
14 Peiris JSM, Tang WH, Chan KH, et al. Children with respiratory disease associated with metapneumovirus in Hong Kong. *Emerg Infect Dis* 2003; **9:** 628–33.
15 PCR primers for SARS developed by WHO network laboratories. http://www.who.int/csr/sars/primers/en/ (accessed July 8, 2003).
16 Stephensen CB, Casebolt DB, Gangopadhyay NN. Phylogenetic analysis of a highly conserved region of the polymerase gene from 11 coronaviruses and development of a consensus polymerase chain reaction assay. *Virus Res* 1999; **60:** 181–89.
17 Peret TCT, Boivin G, Li Y, et al. Characterization of human metapneumoviruses isolated from patients in North America. *J Infect Dis* 2002; **185:** 1660–63.
18 Chan PKS, Tam JS, Lam CW, et al. Detection of human metapneumovirus from patients with severe acute respiratory syndrome: a methodological evaluation. *Emerg Infect Dis* (in press).
19 Fouchier RA, Bestebroer TM, Herfst S, Van Der KL, Rimmelzwaan GF, Osterhaus AD. Detection of influenza A viruses from different species by PCR amplification of conserved sequences in the matrix gene. *J Clin Microbiol* 2000; **38:** 4096–101.
20 Lai MMC, Holmes KV. *Coronaviridae*: the viruses and their replication. In: Knipe DM, Howley PM, eds. Fields virology. Philadelphia: Lippincott Williams and Wilkins, 1999: 1163–85.
21 Claas HC, Melchers WJG, De Bruijn IH, et al. Detection of *Chlamydia trachomatis* in clinical specimens by the polymerase chain reaction. *Eur J Clin Microbiol Infect Dis* 1990; **9:** 864–68.
22 Reischl U, Lehn N, Simnacher U, Marre R, Essig A. Rapid and standardised detection of *Chlamydia pneumoniae* using LightCycler real-time fluorescence PCR. *Eur J Clin Microbiol Infect Dis* 2003; **22:** 54–57.
23 Mahy BWJ. A dictionary of virology, 2nd edn. San Diego: Academic Press, 1997.
24 van den Hoogen BG, de Jong JC, et al. A newly discovered human metapneumovirus isolated from young children with respiratory tract disease. *Nat Medicine* 2001; **7:** 719–24.
25 Bhatt PN, Jacoby RO. Experimental infection of adult axenic rats with Parker's rat coronavirus. *Arch Virol* 1977; **54:** 345–52.
26 O'Toole D, Brown I, Bridges A, Cartwright SF. Pathogenicity of experimental infection with 'pneumotropic' porcine coronavirus. *Res Vet Sci* 1989; **47:** 23–29.
27 Myers JL, Colby TV, Yousem SA. Common pathways and patterns of injury. In: Dail DH, Hammar SP, eds. Pulmonary pathology. New York: Springer-Verlag, 1993: 57–77.
28 Dungworth DL. The respiratory system. In: Jubb KVF, Kennedy PC, Palmer N, eds. Pathology of domestic animals, vol 2. San Diego: Academic Press, 1993: 539–699.
29 Jabrane A, Girard C, Elazhary Y. Pathogenicity of porcine respiratory coronavirus isolated in Québec. *Can Vet J* 1994; **35:** 86–92.
30 Schneider-Schaulies S, ter Meulen V. Measles virus and immunomodulation: molecular bases and perspectives. *Expert Rev Mol Med* 2002; http://expertreviews.org/02004696h.htm.

For personal use. Only reproduce with permission from The Lancet.